Reproductive isolation among lineages of Silene nutans (Caryophyllaceae): A potential involvement of plastid-nuclear incompatibilities

Zoé Postel, Céline Poux, Sophie Gallina, Jean-Stéphane Varré, Cécile Godé, Eric Schmitt, Etienne Meyer, Fabienne van Rossum, Pascal Touzet

Molecular Phylogenetics and Evolution 169 (2022) 107436

Contents lists available at ScienceDirect

Molecular Phylogenetics and Evolution

journal homepage: www.elsevier.com/locate/ympev

Reproductive isolation among lineages of *Silene nutans* (Caryophyllaceae): A potential involvement of plastid-nuclear incompatibilities

Zoé Postel [a], Céline Poux [a], Sophie Gallina [a], Jean-Stéphane Varré [b], Cécile Godé [a], Eric Schmitt [a], Etienne Meyer [c], Fabienne Van Rossum [d,e], Pascal Touzet [a,*]

[a] Univ. Lille, CNRS, UMR 8198 - Evo-Eco-Paleo, F-59000 Lille, France
[b] Univ. Lille, Inria, UMR CNRS 9189 - CRIStAL Centre de Recherche en Informatique Signal et Automatique de Lille F-59000 Lille, France
[c] Institute of Plant Physiology, Martin-Luther-University, Halle-Wittenberg, Germany
[d] Meise Botanic Garden, Nieuwelaan 38, BE-1860 Meise, Belgium
[e] Service général de l'Enseignement supérieur et de la Recherche scientifique, Fédération Wallonie-Bruxelles, rue A. Lavallée 1, BE-1080 Brussels, Belgium

ARTICLE INFO

Keywords:
Coevolution
Cytochrome b6/f
Plastid-nuclear incompatibilities
Ribosome
Plastome
Reproductive isolation
Silene nutans

ABSTRACT

Early stages of speciation in plants might involve genetic incompatibilities between plastid and nuclear genomes, leading to inter-lineage hybrid breakdown due to the disruption between co-adapted plastid and nuclear genes encoding subunits of the same plastid protein complexes. We tested this hypothesis in *Silene nutans*, a gynodioecious Caryophyllaceae, where four distinct genetic lineages exhibited strong reproductive isolation among each other, resulting in chlorotic or variegated hybrids. By sequencing the whole gene content of the four plastomes through gene capture, and a large part of the nuclear genes encoding plastid subunits from RNAseq data, we searched for non-synonymous substitutions fixed in each lineage on both genomes. Lineages of *S. nutans* exhibited a high level of dN/dS ratios for plastid and nuclear genes encoding most plastid complexes, with a strong pattern of coevolution for genes encoding the subunits of ribosome and cytochrome b6/f that could explain the chlorosis of hybrids. Overall, relaxation of selection due to past bottlenecks and positive selection have driven the diversity pattern observed in *S. nutans* plastid complexes, leading to plastid-nuclear incompatibilities. We discuss the possible role of gynodioecy in the evolutionary dynamics of the plastomes through linked selection.

1. Introduction

Speciation, the process that leads populations to reproductive isolation is a main topic of investigation in evolutionary genetics (Matute and Cooper, 2021). The involvement of cytonuclear interactions in the emergence of reproductive barriers has long been underestimated (Levin, 2003). However, the asymmetry of reproductive isolation when hybrids from reciprocal crosses are compared, the so-called Darwin's corollary, suggests a possible cytoplasmic origin of genetic incompatibilities (Burton et al., 2013; Turelli and Moyle, 2007). In fact, cytonuclear incompatibilities might contribute to early stages of speciation (Barnard-Kubow et al., 2017). Several studies in plant species have pointed out the role of plastid-nuclear incompatibilities in post-zygotic isolation (Bogdanova, 2020; Postel and Touzet, 2020). Due to the dual origin of plastid protein complexes (plastid and nuclear), any mutation fixed in one genome through adaptive or non-adaptive processes is expected to trigger the selection on partner genome to maintain co-adaptation and a functional plastid (Greiner and Bock, 2013). The pattern of coevolution between plastid and nuclear genes involved in the same plastid complexes is indeed strong (Forsythe et al., 2021) and could subsequently generate incompatibilities between divergent lineages revealed by hybrid breakdown. Hybrid breakdown can be associated with chlorosis, reduced plant fitness, fertility, and survival (Greiner et al., 2011). For most cases, the molecular mechanism behind this breakdown is unknown, with the exception of evening primroses (*Oenothera* spp.), where a recent study has demonstrated the involvement of a photosynthesis operon, the expression of which is most likely involved in light acclimation (Zupok et al., 2021).

In the present study, we aimed to assess the possible involvement of plastid-nuclear incompatibilities in *Silene nutans* L. (Caryophyllaceae), a perennial, moth-pollinated herb species from xero-thermophilous habitats showing a wide continental Eurasian distribution. Population

* Corresponding author.
E-mail address: pascal.touzet@univ-lille.fr (P. Touzet).

https://doi.org/10.1016/j.ympev.2022.107436
Received 10 August 2021; Received in revised form 28 January 2022; Accepted 2 February 2022
Available online 4 February 2022

genetic studies have revealed the occurrence of several distinct genetic lineages based on plastid sequences and nuclear microsatellite markers, whose geographic distribution in Europe reflects colonization from past glacial refugia (Martin et al., 2016; Van Rossum et al., 2018). Diallelic crosses between four of these lineages, one from the eastern part of *S. nutans* distribution (E1) and three found in Western Europe (W1, W2, and W3), revealed strong reproductive isolation between them (Martin et al., 2017; Van Rossum et al., unpublished results). This reproductive isolation depends on the direction of the cross in reciprocal crosses (i.e., is asymmetrical) and results in chlorotic or variegated hybrids with a high level of mortality or reduced plant fitness at the juvenile stage.

To assess whether hybrid breakdown between E1, W1, W2, and W3 genetic lineages of *S. nutans* involves plastid-nuclear incompatibilities, we searched for non-synonymous substitutions in plastid and nuclear genes encoding plastid protein subunit complexes, which are specifically fixed in lineages. We did so by analyzing the whole gene content of the

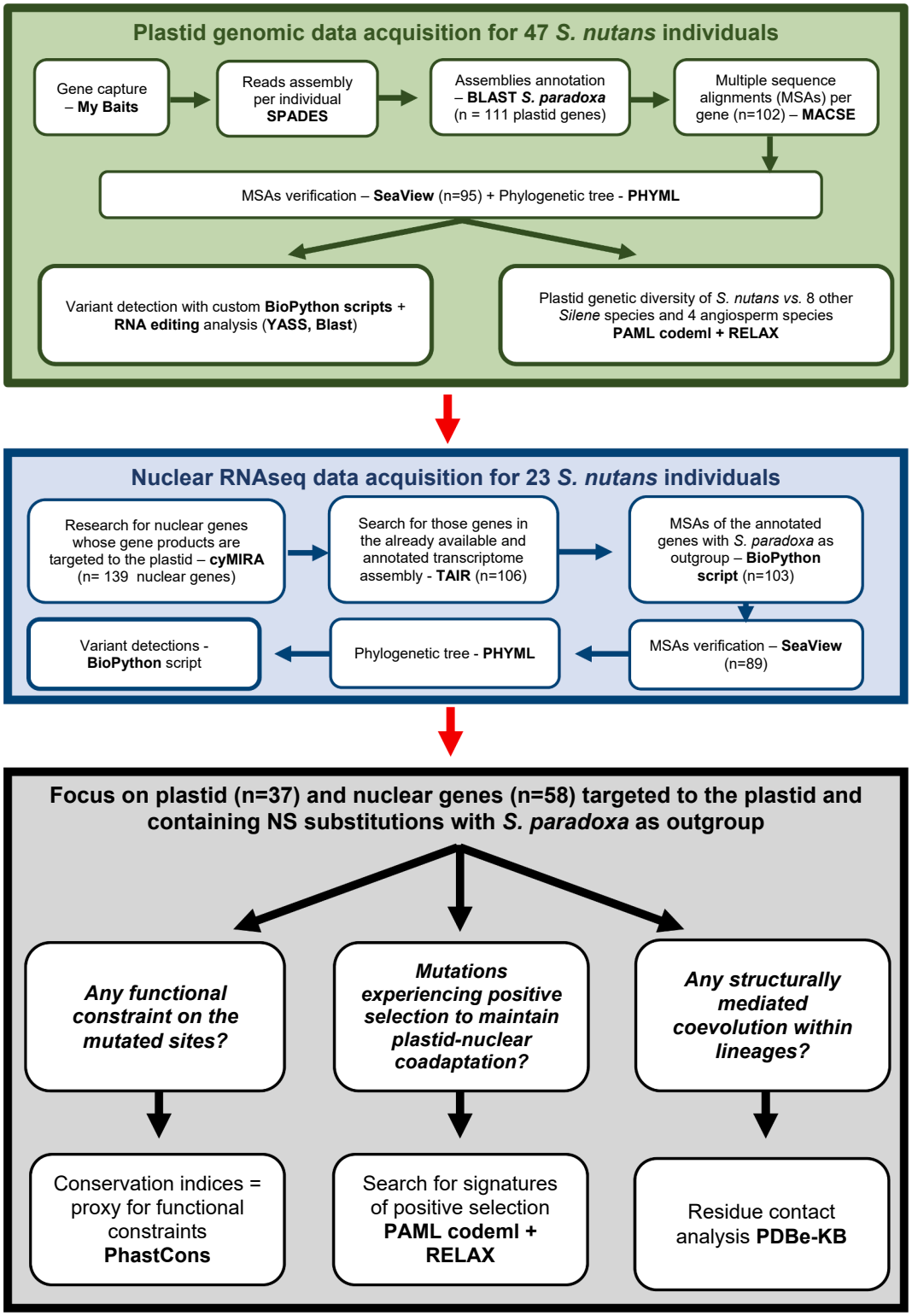

Fig. 1. Summary of the methods used for detecting plastid-nuclear incompatibilities between lineages of *S. nutans*.

four plastomes, and most of the nuclear genes encoding subunits of plastid complexes. We then estimated the functional effect of these non-synonymous substitutions (through a conservation index and their role in contacts between subunits within complexes) as well as whether they exhibited a signature of relaxed or positive selection. Finally, we discuss the different scenarios that could have favored the emergence of plastid-nuclear incompatibilities in *S. nutans*.

2. Material and methods

The overall workflow is summarized in Fig. 1.

2.1. Plastid genomic data

To acquire plastid genomic data of *S. nutans*, 47 individuals from 24 populations (1–2 individuals per population) from UK, France, Belgium, Luxemburg, Germany, and Finland (Table S1) were sampled from the DNA collection of the unit Evo-Eco-Paleo (UMR 8198 – CNRS University of Lille; see Martin et al., 2016 for DNA extraction procedure) (Table S1). These populations covered four genetic lineages of *S. nutans* based on plastid SNP markers (Martin et al., 2016), with 12 individuals belonging to E1 and W1 lineages and eight individuals to W2 and W3 lineages. Genomic sequences for each individual were obtained through gene capture with a myBaits® target capture kit (Daicel Arbor Biosciences, https://arborbiosci.com/). DNA probes were defined from the published sequence of the plastid genome of *Silene latifolia* (NCBI accession: Cl_001 – NC_016730.1). In order to get 1 Mbp per sample with a theoretical coverage of 50X, 4255 probes of 120 nucleotides long were defined for a total target length of 267156 bp with a 2x density (i.e. 534328 bp). Enriched libraries were pooled and sequenced on Illumina MiSeq in paired-end (2 × 150 of the 48 genomic libraries for our sample, in dual index kappa) at the LIGAN platform (UMR 8199 LIGAN-PM Genomics platform – Lille, France), resulting in a total of 38 million reads. De novo assemblies of the reads were generated using SPAdes (Bankevich et al., 2012). Their quality was assessed by YASS (Noé and Kucherov, 2005) and Blast analyses (Table S2).

Multiple sequence alignments (MSAs) were generated using *Silene paradoxa* plastid genome assembly (NCBI accession: NC_023360.1), which was not available when the baits were defined and was phylogenetically closer to *S. nutans* (Jafari et al., 2020). The 111 gene sequences of *S. paradoxa* were blasted against the assemblies of *S. nutans* individuals and the best hit for each gene was extracted. For two genes, *clpP* and *trnK-UUU*, no hits were detected. Blast results were then filtered for a percentage of identity of 90% and a length of 30 bp to also get the small *trn* genes. After filtration, we conserved 103 genes out of the 111 annotated in *S. paradoxa* plastid genome. The gene *ycf1* was also excluded because it was missing in more than 50% of our samples. With the program MACSE 2.00 (Ranwez et al., 2011), MSAs of the blasted plastid genes were generated and aligned, containing the sequences of *S. latifolia, S. paradoxa*, and of the 47 sampled individuals of *S. nutans*. MSAs were manually cleaned and checked on SeaView 4.7 (Gouy et al., 2010). Seven genes were excluded following this step, depending on the quality of the alignment and the correct frame of the ORFs (i.e., *accD, atpF, rpoC1, rps12, trnT-GGU*, *ycf2*, and *ycf3*). Among the remaining 95 plastid genes, 23 were *trn* genes and four were *rrn* genes which were not analyzed here. A phylogenetic tree was generated with PHYML 3.0 (Guindon et al., 2010) with the concatenated set of the 68 genes, using the GTR + GAMMA model of nucleotide substitution selected by SMS (*Smart Model Selection*) (Lefort et al., 2017).

To compare the evolutionary trends of *S. nutans* plastid genomes, we constructed MSAs including 10 other angiosperm and *Silene* species for which plastid genome assemblies were available on NCBI: *Arabidopsis thaliana* (NC_000932), *Nicotiana tabacum* (NC_001879), *Oryza sativa* (NC_001320), and *Zea mays* (NC_001666), and for *Silene* species: *S. capitata* (NC_035226.1*), S. chalcedonica* (NC_023359.1), *S. conica* (NC_016729.1), *S. conoidea* (NC_023358.1), *S. noctiflora* (NC_012728.1), and *S. vulgaris* (NC_016727.1). Plastid gene sequences of *S. nutans* individuals were blasted against plastome assemblies of these species (percentage of identity of 98%) and the best blast hit was extracted. To avoid bias due to the larger amount of data for *S. nutans* lineages, MSAs were constructed for the 68 plastid genes with only one sequence per *S. nutans* lineage. To choose which individual to keep for this analysis, we selected the individual with the least fragmented assembly within each lineage. MSAs with *Silene* and angiosperm species nucleotide sequences were aligned with MUSCLE and manually checked on SeaView. Concatenations were generated per plastid complex: photosystem I and II (PSI and PSII), ATP synthase, cytochrome b6/f, Rubisco, NDH, RNA polymerase, and large and small ribosomal subunits (LSU and SSU, respectively), except for three genes (*ccsA, cemA* and *matK*). For all concatenations, phylogenetic trees were generated using PHYML 3.0 with the GTR model of nucleotide substitutions selected by SMS.

2.2. Nuclear data

To identify nuclear genes potentially involved in plastid-nuclear incompatibilities (PNIs), we searched for nuclear genes encoding subunits of plastid complexes. We used the protein-protein interaction database cyMIRA (Forsythe et al., 2019), the Protein Data Bank in Europe-Knowledge Base (PDBe-KB) (Varadi et al., 2020), SUBA4 (Hooper et al., 2017), UniProt (Bateman, 2019), STRING 11 (Szklarczyk et al., 2019), and BioGrid (Oughtred et al., 2019) to establish a list of 139 putative nuclear interactors (Table S3).

A transcriptome assembly was already available as well as transcriptomic data for 22 individuals from the four genetic lineages of *S. nutans* (Table S1) (Muyle et al., 2021; PRJEB39526). RNAs were extracted from flower buds. An in-house BioPython script was used to align the reads of these 22 individuals on the transcriptome assembly. We used BamBam (SAMtools package) (Page et al., 2014) to generate one consensus sequence per individual from the reads. From this, we extracted the nuclear genes identified and annotated in the transcriptome, using their position in the transcriptome assembly and their TAIR identifiers. Only 106 out of the 139 nuclear genes were found in *S. nutans* transcriptomes and were subsequently analyzed. MSAs per gene containing *S. nutans* individuals were blasted on *S. latifolia* and *S. paradoxa* transcriptomes (PRJEB39526), using the same criteria as for plastid genes, extracting the best hits for both species. Three nuclear genes for which no hits were identified in *S. latifolia* or *S. paradoxa* were excluded. The MSAs for the 103 remaining nuclear genes were then aligned with MUSCLE and checked on SeaView. Fourteen genes for which alignment with a correct ORF was not possible were excluded. A concatenated set of 89 nuclear genes was generated to construct a phylogenetic tree using PHYML 3.0 with the GTR model of nucleotide substitution selected by SMS. As with the plastid data, we constructed nuclear gene concatenation per plastid complex.

To compare evolutionary patterns of nuclear genes encoding subunits of the plastid ribosome with the nuclear genes encoding subunits of the cytosolic ribosome (i.e., gene products not targeted to the plastid), RNAseq data for these genes were also extracted and aligned. We took the 204 nuclear genes used in Sloan et al. (2014a) and their available TAIR identifiers. The same steps as described above were followed, and MSAs containing the sequences of the 22 *S. nutans* individuals, *S. paradoxa,* and *S. latifolia* were generated for 81 genes. Indeed, only 87 out of 204 genes were found in the transcriptomic data, five of which did not show any blast hits with *S. paradoxa* and *S. latifolia* transcriptomes, and one of which it was not possible to construct an alignment with a correct ORF.

2.3. Variant detection

We used an in-house BioPython script to identify the SNPs (single nucleotide polymorphisms) differing between the four lineages in the MSAs of the 95 plastid genes. As RNAseq data of *S. nutans* were available

(Muyle et al., 2021), we also checked whether the identified non-synonymous substitutions were "true non-synonymous substitutions" or RNA editing sites (T to C substitutions) using RNAseq data and confirmed that they were non-edited (see Appendix S1).

For the nuclear genes, the diploid individual genotypes were determined at each position in the individual alignment with the program reads2spn (Gayral et al., 2013) and used to identify the nuclear variants. An in-house BioPython script was used to identify the SNPs only present in one lineage. Only SNPs for which at least two individuals per lineage were genotyped were kept. To determine non-synonymous or synonymous nature of the identified SNPs, we used the available assembly of *S. nutans* transcriptome, for which ORFs were set.

2.4. Conservation status analysis

First, to improve the accuracy of the analysis, additional outgroups were added to the existing nuclear MSAs. We used the transcriptome assemblies of *Dianthus chinensis, S. diclinis, S. dioica, S. heuffelli, S. latifolia, S. marizii, S. otites*, *S. paradoxa*, S. *pseudotites, S. viscosa*, and *S. vulgaris* (Muyle et al., 2021). Nuclear gene sequence data were extracted from these transcriptomes and new MSAs were constructed, integrating the sequences of those species. For the plastid genes, the analysis was run on the 12 species used for the plastid genetic diversity analysis. Then, for both nuclear and plastid data, a phylogenetic tree was constructed using the concatenated set of the nuclear and plastid genes, respectively, with PHYML – SMS, which assessed the best model of nucleotide substitutions to use.

We then estimated the conservation degree of the mutated amino acids as a proxy for the functional constraint acting on the mutated sites of the plastid and nuclear genes using the PHAST program (Hubisz et al., 2011). For this purpose, we ran PhyloFit analyses to fit a phylogenetic model to the MSA by maximum likelihood (Siepel and Haussler, 2004), using HKY85 as a model of nucleotide substitutions and the EM option. With the phylogenetic model output file of PhyloFit, we ran PhastCons a first time as a training step to estimate PhastCons free parameters as suggested in Hubisz et al. (2011) (option – *no-post-probs*). Then, we ran PhastCons a second time with the formerly estimated parameters, to compute the conservation scores for each nucleotide site in a given MSA, varying from 0 = poorly conserved to 1 = strongly conserved. These three steps were conducted for each MSA.

2.5. Analysis of the pattern of selection

For assessing the evolutionary dynamics and selection patterns on nuclear and plastid genes in *S. nutans*, we estimated the d_N/d_S ratios, with d_N = non-synonymous substitution rate and d_S = synonymous substitution rate using codeml implemented in PAML 4.9 (Yang, 2007). We ran different analyses with several models. For nuclear genes, as transit peptides of the proteins targeted to the plastid are highly variable and thus could increase d_N/d_S ratios (Christian et al., 2020), we used the TargetP software (Juan et al., 2019) to identify their locations in the nuclear sequences and remove them from the nuclear alignments.

Two types of analyses have been conducted with codeml, varying in terms of their assumptions about how d_N/d_S varies across the sequence (site models) or across branches of the phylogeny (branch models). Branch models were used to compare the d_N/d_S ratios of *S. nutans* lineages with those of other *Silene* and angiosperm species. These analyses were conducted on the plastid gene concatenations per plastid complex, with the angiosperms and *Silene* species as outgroups (Figure S1, Appendix S2). Compensatory mutations could be a target of positive selection for the maintenance of the interactions between plastid and nuclear gene partners. To detect signatures of positive selection, either on specific non-synonymous substitution sites or on particular genes, site models were run on plastid and nuclear genes alignments, with only *S. latifolia* and *S. paradoxa* as outgroups. Separated analyses were run for the plastid and nuclear ribosome genes and the 81 nuclear genes encoding the cytosolic ribosome (i.e., not targeted to the plastid, later called NuCyto) (Appendix S2). For each analysis, the d_N/d_S values of the best models were kept. To test for differences in d_N/d_S values on plastid vs. nuclear genes and on nuclear genes encoding the plastid ribosome vs. NuCyto, we performed Mann-Whitney *U* tests on R 1.3.1093 (package *stats4*).

A second analysis of selection with RELAX (Wertheim et al., 2015) was performed to assess selective pressures acting on nuclear and plastid genes in *S. nutans*. RELAX allows to distinguish positive selection from relaxed purifying selection in case of elevated d_N/d_S ratios. We used the program RELAX with default parameters values. We used the same dataset as for the codeml analyses: first the plastid gene concatenations with the angiosperm and *Silene* species and then the plastid and nuclear gene alignments, with only *S. latifolia* and *S. paradoxa*. For both datasets, the outgroups were annotated as references branches and *Silene nutans* individuals were again annotated as test branches, for both nuclear and plastid genes.

Finally, to test for the parallel pattern of mutation accumulation between plastid and nuclear genes of *S. nutans* lineages, we performed a Spearman's rank correlation analysis between p_N/p_S ratios of plastid and nuclear gene concatenations per complex on *S. nutans dataset*. We used DNAsp 6 (Rozas et al., 2017) to calculate p_N and p_S values, i.e., non-synonymous and synonymous divergences, respectively, between *S. nutans* lineages.

2.6. Identification of contact positions in plastid complexes

To assess whether some non-synonymous substitutions identified in plastid and nuclear genes were located at contact positions in the plastid complexes, we conducted a residue contact analysis, using crystallographic structures of the different plastid complexes. The PDBe-KB references of the plastid complexes were extracted from cyMIRA database (Forsythe et al., 2019). When the crystallographic structure of the plastid complex was available, we extracted the protein sequences of the organism with which the crystallographic structures had been defined and aligned them with the protein sequences of the *S. nutans* individuals. Data were not available for RNA polymerase and Rubisco.

3. Results

3.1. Genomic and transcriptomic data

Plastid genome assemblies in *S. nutans* were relatively fragmented as they were composed of six nodes on average, with a minimum of three nodes for individuals AIG-1 and AIG-10 (W3 lineage) and a maximum of 23 for individual UK15-16 (W1 lineage). The data obtained represent between 86.25% (W2) and 96.63% (E1) of the complete *S. latifolia* plastid genome (Table S2). Compared with the plastid genome of *S. paradoxa*, most of the genes of the plastid complexes were recovered, with only a few plastid complexes lacking one gene (ATP synthase, NDH, RNA polymerase, and large and small ribosomal subunits) (Table 1). As for the plastid genome, about 75% of the nuclear genes annotated in the *S. paradoxa* transcriptome whose gene products were targeted to the plastid found a blast hit in *S. nutans* transcriptomic assemblies (Table 1, Table S3). Nonetheless, compared to the plastid genomes, nuclear gene annotation was less complete, most likely depending on the level of gene expression in flower buds.

3.2. Plastid genome diversity in Silene nutans

Variant analyses revealed that a high proportion of the annotated plastid genes were variable (72.1%), containing synonymous or non-synonymous substitutions (Table 1). The number of synonymous substitutions (66) was lower than the number of non-synonymous substitutions (139). All the plastid complexes contained plastid genes with mutated sites, especially the plastid genes encoding the expression

Table 1
Summary of the plastid and nuclear genetic diversity per plastid complex.

Plastid Complex	Genome	Number of genes				Gene concatenations length (in bp)	Number of synonymous substitutions	Number of non-synonymous substitutions			
		Total	Annotated	Analyzed	Variable			Total	Conserved positions	Positive selection	Residue contact
PSI	Plastid	5	5	5	2	5355	7	1	1	0	0
	Nuclear	20	16	14	8	10,624	17	10	0	0	1
PSII	Plastid	15	15	15	7	6672	18	5	5	0	0
	Nuclear	28	19	17	10	11,107	4	32	0	2	0
Rubisco	Plastid	1	1	1	1	1425	1	0	0	NA	NA
	Nuclear	4	1	1	1	1095	1	4	0	0	0
ATP synthase	Plastid	6	6	5	4	4375	3	6	3	0	0
	Nuclear	6	5	4	3	2858	3	6	1	0	0
Cyb6F	Plastid	6	6	6	2	2362	1	3	2	0	0
	Nuclear	4	4	4	4	3440	3	18	2	9	1
NDH	Plastid	11	11	11	7	10,370	8	17	10	1	1
	Nuclear	18	11	5	1	2472	1	1	0	0	0
RNA polymerase	Plastid	4	4	3	3	8279	11	17	9	2	0
	Nuclear	10	10	7	5	5654	1	8	1	0	2
LSU	Plastid	9	9	8	8	2338	6	34	19	1	8
	Nuclear	30	24	22	17	12,606	16	56	10	7	4
SSU	Plastid	12	11	10	7	4077	6	44	16	5	8
	Nuclear	12	10	10	8	6623	8	40	12	10	6
Others	Plastid	9	8	4	4	3157	5	12	7	0	NA
	Nuclear	NA	6	4	4	4449	5	9	1	2	NA
Total	Plastid	78	76	68	45	x	66	139	74	9	17
	Nuclear	139	106	88	61	x	63	180	27	30	14

Number of genes: Total: the total number of genes annotated in the plastid complex (references taken on PDBe-KB). Trn and rrn genes were not taking into account here; Annotated: number of annotated genes in the S. nutans plastid genomes and transcriptomes; Analyzed: number of genes analyzed per genome and plastid complex; Variable: number of variable genes per genome in each plastid complex; Total: total number of NS substitutions per genome and plastid complex; Conserved positions: number of NS substitutions located at strongly conserved positions (i.e. conservation indice > 0.8); Positive selection: number of NS substitutions identified under positive selection with PAML NSites model.

machinery, i.e., the large and small ribosomal subunits and the RNA polymerase subunits (24.5%, 31.7%, and 12.2% of the total number of non-synonymous substitutions were found in these three complexes, respectively). On average, half of the identified non-synonymous substitutions were located at strongly conserved positions (i.e., conservation index > 0.8), and most of these substitutions were found in the nucleotide sequences of the plastid genes encoding components of the plastid ribosome (Table 1). For these genes, some of the non-synonymous substitutions were located at strongly conserved positions (19/34 encoding the LSU and 16/44 encoding the SSU), and among them, some led to a change in the functional class of the encoded amino-acid (4/19 for the LSU and 8/16 for the SSU). These plastid genes also contained 94% of the non-synonymous substitutions located at residue contact positions (i.e., eight substitutions for both large and small ribosomal subunit) (Table 1). The synonymous substitutions exhibited contrasting patterns of accumulation. An overrepresented portion of these substitutions (27.3%) was located in the genes encoding subunits of the photosystem II and very few substitutions were identified in the genes involved in the plastid gene expression machinery (Table 1).

Overall, *S. nutans* lineages exhibited the highest d_N/d_S ratios in the gene concatenations of plastid complexes compared with other *Silene* and angiosperm species (Fig. 2), even with *Silene* species known to exhibit accelerated rates of organellar genome evolution (*S. conica*, *S. conoidea*, and *S. noctiflora*). For these species, elevated d_N/d_S ratios were only observed in the large and small ribosomal subunits (Sloan et al., 2014a). In *S. nutans,* not only did gene concatenation of these two subunits have elevated d_N/d_S ratios (>1), but this was also observed for all plastid complexes, especially in W2 and E1 lineages, and for the plastid genes encoding the cytochrome b6/f (Fig. 2). Indeed, the latter exhibited the highest d_N/d_S ratio among the plastid genes encoding complexes involved in photosynthesis and compared to angiosperm and other *Silene* species. The particular case of *S. paradoxa* must be noted, with a median d_N/d_S ratio slightly higher than W1 and W3 lineages (Fig. 2).

Using RELAX, we identified a tendency for relaxed purifying selection on the plastid genes encoding the plastid complexes of *S. nutans* (Fig. 2). For large and small ribosomal subunits, showing d_N/d_S ratios > 1, RELAX results identified intensification of positive selection on their plastid genes (Fig. 2).

3.3. Analyses of nuclear genes encoding subunits of plastid complexes

As observed on plastid genes, more than half (57.5%) of the nuclear genes annotated in *S. nutans* lineage transcriptomes contained synonymous or non-synonymous substitutions. The number of synonymous substitutions identified in nuclear genes was also lower than the amount of non-synonymous substitutions, and the difference between the number of synonymous and non-synonymous substitutions in nuclear genes was higher than for plastid genes (63 synonymous and 180 non-synonymous substitutions in nuclear genes vs. 66 synonymous and 139 non-synonymous substitutions in plastid genes; Table 1). Nuclear genes encoding products targeted to the plastid accumulated more non-synonymous substitutions than the plastid ones. Despite some specificities to each genome (i.e., substitutions in NDH complex for plastid genes vs. in cytochrome b6/f and photosystem II for nuclear genes), the accumulation patterns of the nuclear and plastid non-synonymous substitutions were similar. Most of the non-synonymous substitutions were located in the nuclear genes encoding subunits of the plastid ribosome (>50% of them) and the RNA polymerase (Table 1). For these nuclear genes, 22/96 non-synonymous substitutions led to changes of amino-acid functional class (i.e., 17 for the genes encoding the SSU and five for the LSU). They also contained 71.4% of the substitutions located at residue contact positions (Table 1). For the cytochrome b6/f, non-synonymous substitutions were also identified, especially in the nuclear gene *petM* for which 11/13 substitutions led to changes of amino-acid functional class (Table 1, Table S4).

For non-synonymous substitutions, 15% were located at strongly conserved positions in the nuclear genes, which was less than for the plastid genes (53.2%) (Table 1). These mutations were mostly found in the nuclear genes encoding subunits of the plastid ribosome (81.5%), as observed for the plastid non-synonymous substitutions. The remaining non-synonymous substitutions at strongly conserved sites were identified in the nuclear genes encoding subunits of the cytochrome b6/f, ATP synthase, and RNA polymerase and in nuclear genes with other functions (Table 1).

3.4. Patterns of selection and coevolution

Sites models analyses in codeml pointed out non-synonymous sub-

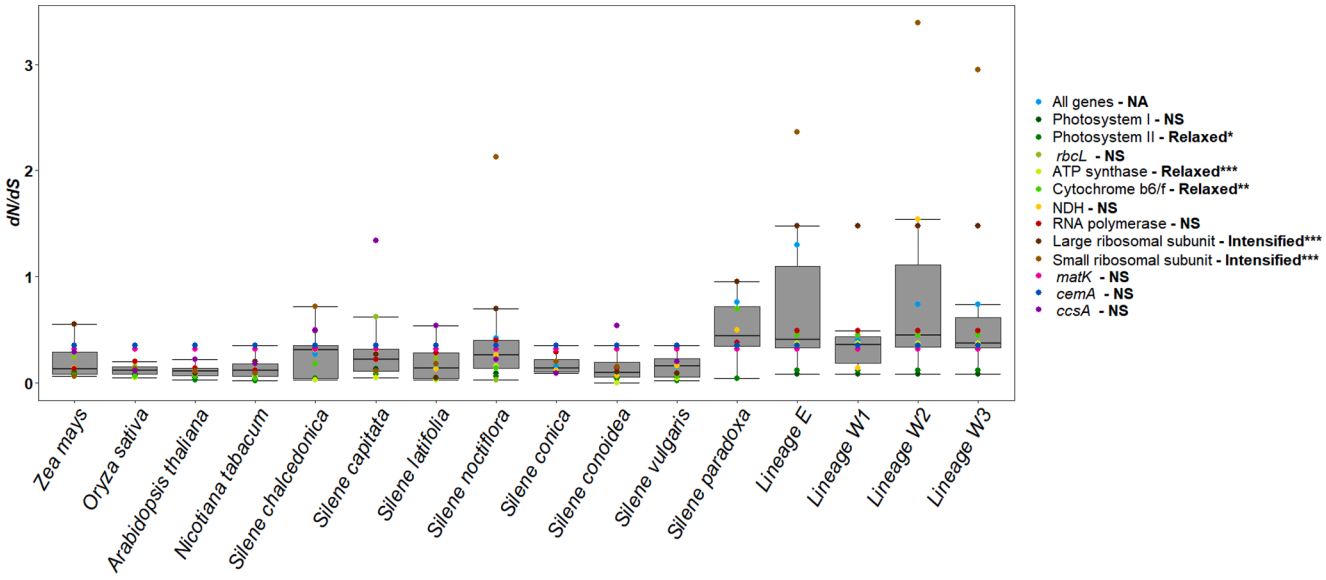

Fig. 2. d_N/d_S ratios of plastid gene concatenations per plastid complex for each lineage of *Silene nutans* and the outgroups used. The first species are the 4 angiosperm species, the next ones regroups the *Silene* species and the last four are the four lineages of *Silene nutans*. RELAX results as well as P value for the plastid gene concatenations of *S. nutans* are given in top right of each graph: ° < 0,1; * < 0,05; ** < 0,01; *** < 0,001; NA = no result for this category due to RELAX own limitations.

stitutions in plastid and nuclear genes under positive selection in *S. nutans* genomes (Table 1). These positively selected mutations mostly concerned genes encoding the large and small ribosomal subunits for both plastid and nuclear compartments and the cytochrome b6/f for the nuclear compartment (23.3%, 40%, and 30% of the nuclear genes, respectively). Overall, nuclear genes encoding the plastid ribosome exhibited 56.7% of the nuclear sites under positive selection. d_N/d_S ratios between nuclear and plastid genes were significantly different for photosystem I (Mann-Whitney *U* tests = 3, P < 0.003), photosystem II (Mann-Whitney *U* tests = 46, P < 0.03), and not significantly different for the rest of the plastid complex gene pairs (P > 0.05) (Fig. 3). We did not find a significant correlation between d_N/d_S ratios of plastid and nuclear gene concatenations encoding the same complexes ($r_s = 0.17$, P = 0.66) but a significant one between p_N/p_S ratios, when focusing on divergence among lineages ($r_s = 0.75$, P = 0.02), suggesting a pattern of coevolution (Figure S2).

d_N/d_S ratios were overall higher for nuclear genes (between 0.2 and 0.3) than for plastid genes (generally < 0.2; Fig. 3), except for the large ribosomal subunit where the reverse pattern was observed. For both nuclear and plastid genomes, elevated d_N/d_S ratios (>1) were observed for some genes encoding subunits of the plastid ribosome (Fig. 3, Table 2). The nuclear genes of cytochrome b6/f also exhibited extremely high d_N/d_S ratios, with $d_N/d_S \approx 2$ for *petM* (Fig. 3, Table 2). Besides, RELAX results were significant and indicated intensification of positive selection for *petM*. The analysis was not decisive for most of the other genes (Table 2, Tables S5 and S6).

In order to formally test the hypothesis of plastid-nuclear coevolution, we calculated d_N/d_S ratios of nuclear genes encoding the subunits of the cytosolic ribosome, i.e., not targeted to the plastid. For the SSU, they showed a d_N/d_S ratio that was ten times lower than the ratio of the nuclear genes encoding the SSU of the plastid ribosome (median value = 0.04 and 0.57, respectively; Fig. 4), and almost 20 times lower than the ratio of the plastid genes encoding the SSU of the plastid ribosome (median value = 0.72). For the LSU of the plastid and cytosolic ribosome, d_N/d_S ratios of the nuclear genes encoding LSU of the cytosolic ribosome was around six and ten times lower than nuclear and plastid genes encoding the LSU of the plastid ribosome, respectively (median value = 0.06, 0.17 and 0.70, respectively; Fig. 4). These differences were significant (Mann-Whitney *U* tests = 173–534, *P* < 0.001). Excess non-synonymous substitutions observed in nuclear genes encoding the plastid ribosome and elevated d_N/d_S ratio (in some case > 1) could thus be driven by plastid-nuclear coevolution within the lineages of *S. nutans*

3.5. Toward the identification of plastid-nuclear gene pairs candidates for PNI

As plastid-nuclear coevolution is expected to be lineage-specific, we looked at patterns of substitution accumulation within the four lineages of *S. nutans* in nuclear and plastid genes. As expected from former studies, phylogenetic relationships between *S. nutans* lineages showed that the western lineages (W1, W2, and W3) clustered together, with the eastern lineage (E1) diverging before the diversification of the western lineages (Martin et al., 2016; Van Rossum et al., 2018) (Fig. 5A). E1 and W2 lineages contained a high number of non-synonymous substitutions in both plastid and nuclear genes: 36 and 55 for E1, and 49 and 44 for W2, respectively (Fig. 5B and C). The W1 lineage exhibited fewer non-synonymous substitutions (17 and 15 for plastid and nuclear genes, respectively). The W3 lineage contained an intermediate number of substitutions in plastid genes (30), but in nuclear genes, it contained as many substitutions as E1 (Fig. 5B and C).

As PNI might be due to the disruption of co-adapted plastid-nuclear gene pairs specific to a given lineage, we focused on gene pairs with non-synonymous substitutions found in conserved sites and exhibiting high levels of d_N/d_S ratios (which can suggest positive selection). In all lineages and for both genomic compartments, the highest number of non-synonymous substitutions concerned the genes encoding the LSU and SSU of the plastid ribosome (ranging from 44.9% of substitutions in plastid genes for W2 to 56.4% of substitutions in nuclear genes for W3; Fig. 5B and C). Most of the fixed substitutions of W1 and W2 lineages were also located in plastid and nuclear genes encoding components of the plastid ribosome (Fig. 5C). This concerned essential plastid-encoded ribosomal genes: *rpl20, rpl22, rpl32, rps2, rps3*, and *rps18* and essential nuclear-encoded ones: *rpl3, rpl13, rpl21, rpl27, rps5, rps9,* and *rps13* (Tiller et al., 2012; Tiller and Bock, 2014). Among the substitutions in

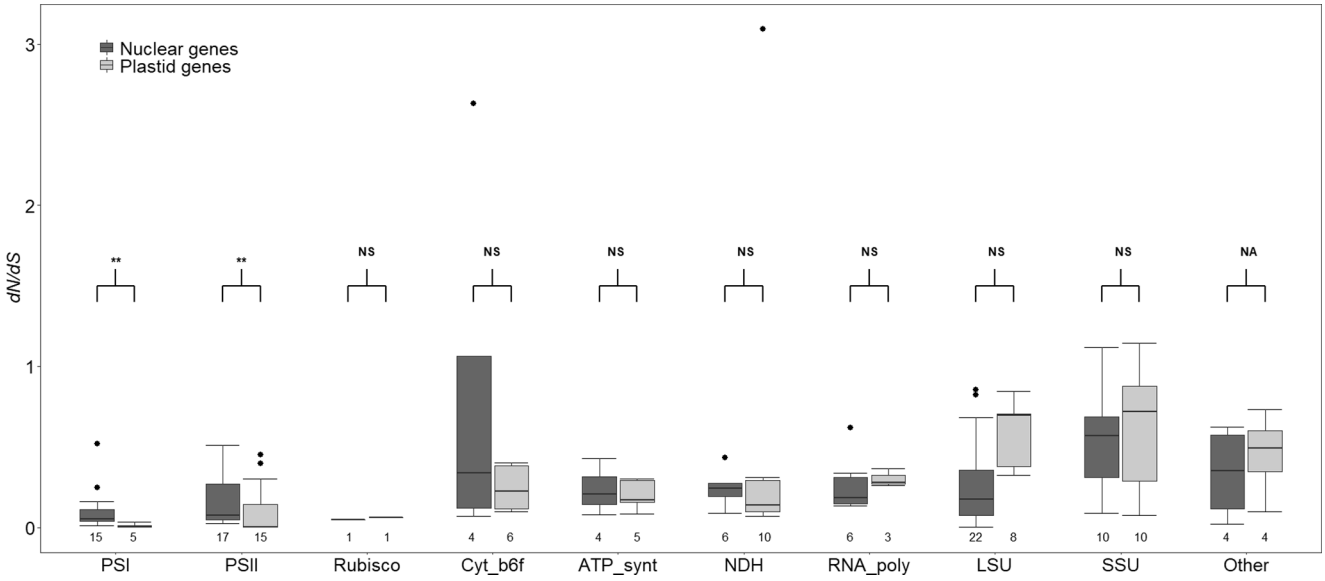

Fig. 3. d_N/d_S ratios calculated on each *S. nutans* gene separately for plastid and nuclear genes encoding plastid complexes. In this analysis all four *S. nutans* lineages display the same d_N/d_S values: branch models analyses with different d_N/d_S ratios for each lineage were significant only for 3 plastid and 14 nuclear genes (data not shown) and exhibited aberrant values (999.99). We have therefore chosen to report the d_N/d_S ratios assessed with the best NSites model (one d_N/d_S ratio for all lineages of *S. nutans*). Overall, d_N/d_S ratios of *S. nutans* were similar between NSites and Branch-Model when a single d_N/d_S ratios was set for all four lineages. Mann-Whitney *U* tests P values: ** = < 0.01; NS = non-significant; NA = no test conducted. The number of analyzed plastid and nuclear genes are reported under each boxplot. PSI: Photosystem I; PSII: Photosystem II; Cyt-B6F: Cytochrome b6/f; ATP_synt: ATP synthase; RNA_polym: RNA polymerase; LSU: Large ribosomal subunit; SSU: Small ribosomal subunit; Other: other functions. Numbers under the boxplots represent the number of genes in each category.

Table 2
dN/dS ratios of the nuclear and plastid genes of the cytochrome b6/f, and of the large and small ribosomal subunits.

Complex	Genome	Gene	dN/dS	Complex	Genome	Gene	dN/dS
Cytochrome b6/f	**Plastid**	*petA*	0.22	**Large ribosomal subunit**	**Plastid**	*rpl2*	0.7
		petB	0.12			*rpl14*	0.33
		petD	0.18			*rpl16*	0.15
		petG	0.00			*rpl20*	0.51
		petL	NA			*rpl22*	1.01
	Nuclear	*DAC*	0.14			*rpl32*	0.50°°
		petC	0.07			*rpl33*	0.7
		petM_1	2.95**			*rpl36*	NA
		petM_2	2.31		**Nuclear**	*EMB3105*	0.12
		PPR	0.54			*PRSP1*	0.68
Small ribosomal subunit	**Plastid**	*rps2*	0.64			*PSRP6*	0.14
		rps3	0.26			*rpl1*	0.21
		rps4	0.29			*rpl3*	0.1
		rps7	NA			*rpl5*	0.32
		rps8	0.08			*rpl6*	0.37
		rps11	0.92			*rpl9*	0.47
		rps14	0.21			*rpl10*	0.05
		rps15	0.73			*rpl11*	0.1
		rps18	NA			*rpl12*	0.03
		rps19	0.73			*rpl13*	0.82
	Nuclear	*PSRP3*	0.65			*rpl15*	0.22°°
		rps1	0.29			*rpl17*	0.02
		rps5	0.62			*rpl18*	0.10
		rps6	1.12**			*rpl19*	0.21
		rps9	0.09			*rpl21*	0.26
		rps10	0.36			*rpl24*	0.07
		rps13	0.7			*rpl27*	0.00
		rps17	0.2			*rpl28*	0.04
		rps20	0.52			*rpl29*	0.5
		rps21	1.83			*rpl31*	0.85

RELAX results: (*) = intensification and (°) = relaxation. P value: * or ° < 0.5; ** or °° < 0.01; *** or °°° < 0.001.

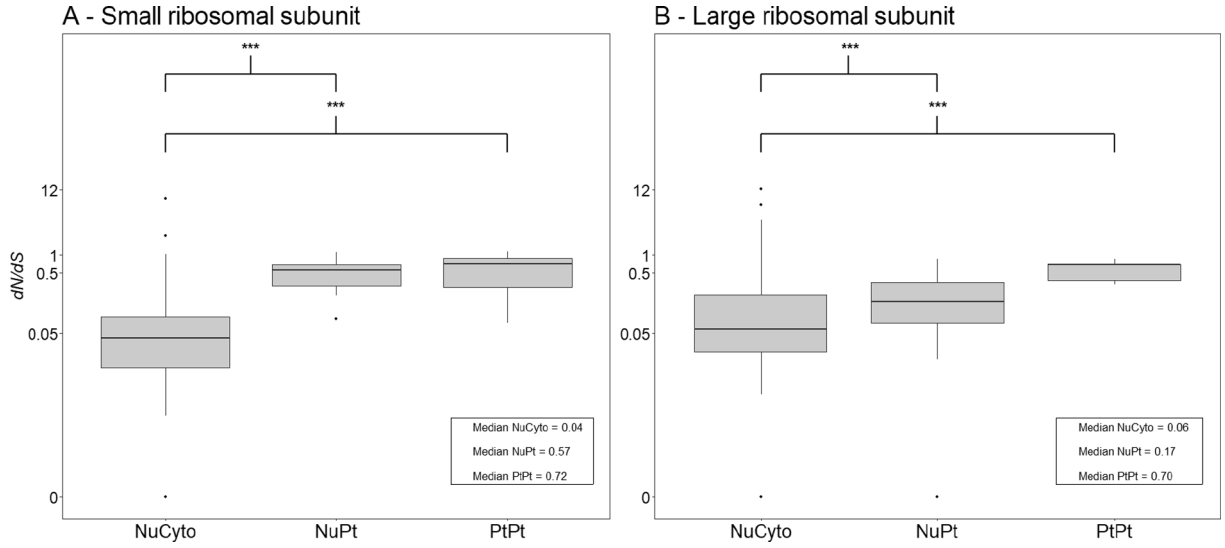

Fig. 4. d_N/d_S ratios calculated on each *S. nutans* gene separately for the plastid and nuclear genes encoding the large (A) and the small (B) SU of the plastid ribosome and for the nuclear genes encoding the cytosolic ribosomes in *S. nutans*. In this analysis all four *S. nutans* lineages display the same d_N/d_S values.d_N/d_S ratios were calculated with codeml (NSites models: one d_N/d_S ratio for all lineage of *S. nutans*). Significant differences in the distributions of d_N/d_S ratios were tested with non-parametric Mann-Whitney *U* tests. NuCyto: Nuclear genes encoding proteins of the cytosolic ribosome. NuPt: Nuclear genes encoding proteins of the plastid ribosome. PtPt: Plastid genes encoding proteins of the plastid ribosome.

these genes, around 50% were in the E1 lineage for the LSU and 30% in the W2 lineage for SSU (Table 1, Tables S7 and S8). RELAX results reported intensification of positive selection in the plastid genes encoding these two complexes with especially elevated d_N/d_S ratios for E1, W2, and W3 lineages (Fig. 2). Some non-synonymous substitutions were identified under positive selection in 1 and 5 plastid genes and in 9 and 7 nuclear genes encoding the LSU and SSU respectively. In particular in the genes *rps3, rps5, rps13*, and *rpl13* which are considered as essential (Tiller et al., 2012; Tiller and Bock, 2014) (Table 1; and see Tables S7 and S8 for details). Among the substitutions under positive selection for the nuclear genes, 66.7% and 71.4% were located in the E1 and W2 lineages, for LSU and SSU, respectively (Tables S7 and S8). Finally, some substitutions either in plastid or in nuclear genes, were identified at residue contact sites, again especially in the genes encoding subunits of the plastid ribosomes (Table 1, Tables S7 and S8).

Nuclear genes of cytochrome b6/f complex, involved in the electron

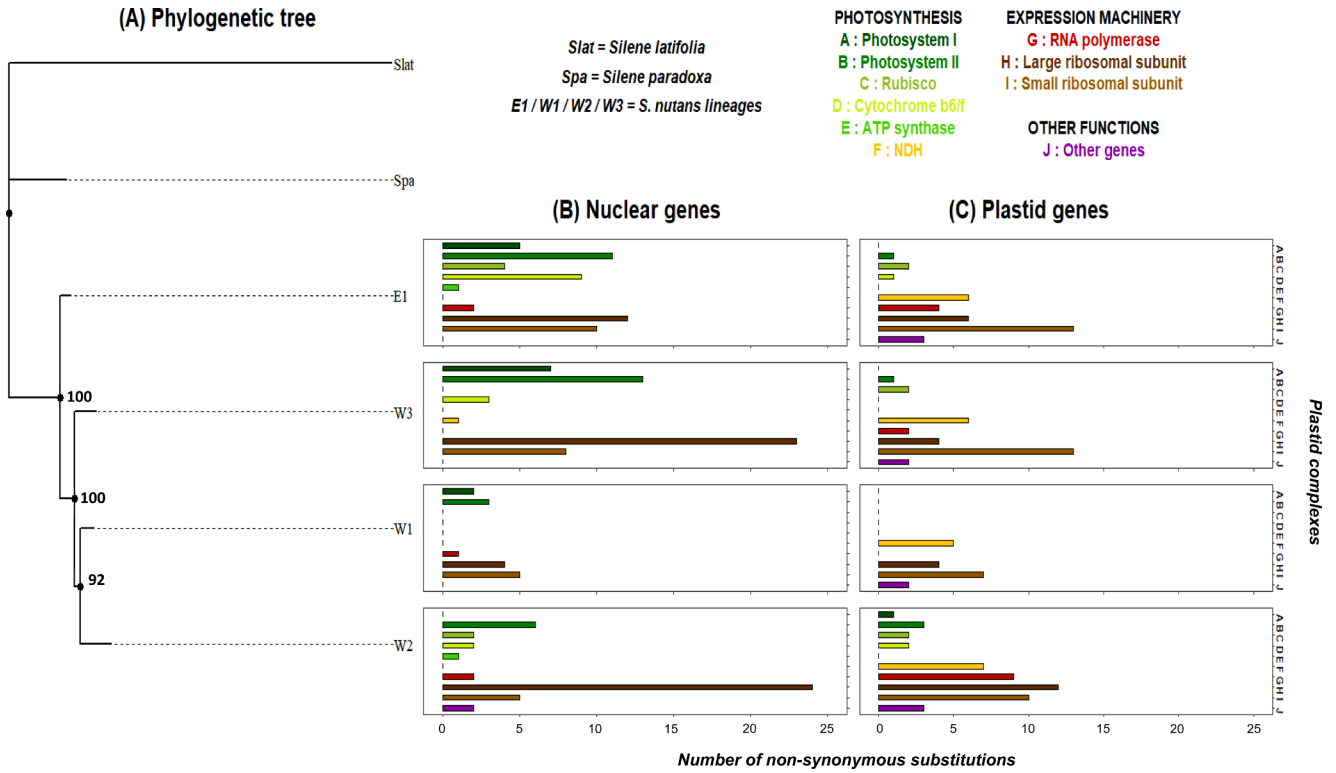

Fig. 5. Non-synonymous substitutions in each lineage of *S. nutans*, per plastid complex. (A) Phylogeny constructed with PHYML based on the concatenated set of the 95 plastid genes, with *S. latifolia* and *S. paradoxa* as outgroups; number of substitutions per plastid complex for the nuclear (B) and plastid (C) genes.

transport chain, also exhibited a large number of mutations, especially in E1 lineage and in *petM*; substitutions were only found in E1 and W2 for the plastid genes encoding subunits of this complex (Figure 6B-C; Table S4). In *petM*, 7/11 non-synonymous substitutions were under positive selection and among them, 5/7 were located in lineages E1 or W2 (Table S4). One substitution was identified at strongly conserved positions in the plastid gene *petA*, in the W2 lineage. Interestingly, *petM* is known as a direct interactor of *petA* (PDBe-KB).

4. Discussion

4.1. Evolution of the plastid genome in Silene nutans

In angiosperms, plastid gene sequences are generally strongly conserved between species (Jansen et al., 2007), partly due to their low mutation rate (Drouin et al., 2008; Wolfe et al., 1987). In the present study, we showed that genetic lineages of *S. nutans* accumulated non-synonymous substitutions in plastid genes. Many mutations were located at strongly conserved positions. These mutations could potentially have an important functional impact, being either deleterious or advantageous. As only a small portion of them showed signatures of positive selection, most of the non-synonymous substitutions located at strongly conserved positions could be at least slightly deleterious. Most plastid complexes exhibited elevated d_N/d_S ratios compared to other *Silene* and angiosperm species, even when considering *Silene* species for which an acceleration of the plastid genome evolution rate has been described (Sloan et al., 2014a). The similar pattern of d_N/d_S ratios found in *S. paradoxa*, although weaker, suggests that similar evolutionary mechanisms could be at stake on the common ancestor of *S. nutans* and *S. paradoxa*. High d_N/d_S values can be the result of positive selection or of relaxed purifying selection. For the plastid genes encoding large and small ribosomal subunits, intensification of selection has been identified for all four genetic lineages of *S. nutans*. These results suggest that intensification of positive selection has played a major role in the excess of non-synonymous substitutions observed for these plastid genes. For the genes encoding other plastid complexes, a tendency for relaxed selection was detected (especially for the plastid genes encoding subunits of the PSII, ATP synthase, cytochrome b6/f, and RNA polymerase).

Either due to positive selection or relaxation of purifying selection, this pattern of mutation accumulation in the plastid genes suggests an accelerated evolutionary rate of the plastid genome in *S. nutans*. Various evolutionary forces could have driven such a pattern. On the one hand, as the plastid genome is a non-recombining genome due to its uniparental mode of inheritance, it has a reduced effective size compared with the nuclear genome (Christie and Beekman, 2017; Greiner et al., 2015). This reduces the efficacy of natural selection and increases the impact of genetic drift on plastid gene sequence evolution (Burton et al., 2013; Greiner and Bock, 2013; Rand et al., 2004). Plastid genome is thus expected to evolve under Muller's ratchet, i.e., a process resulting in an irreversible accumulation of deleterious mutations due to a lack of recombination (Rand et al., 2004). Therefore, the accumulation of non-synonymous substitutions in the plastid genes might be the result of strong genetic drift effects that may have acted when the lineages were isolated from each other in separate refugia in southern and eastern Europe during the last glacial maximum and when populations experienced repeated bottlenecks during postglacial recolonization (Martin et al., 2016; Van Rossum et al., 2018). This might have led to reduced effective sizes and relaxation of purifying selection, increasing the fixation of weakly deleterious mutations (Rockenbach et al., 2016). Conversely, any advantageous mutation occurring within these lineages might also have led to this pattern through linked selection (Cruickshank and Hahn, 2014). Indeed, experimental evidence suggests that cytoplasmic involvement in adaptation has been underestimated (Budar and Roux, 2011). High values of d_N/d_S ratios were also found in reproductively isolated populations of *Campanulastrum americanum*. However, they are lower than the values observed in *S. nutans* lineages (Barnard-Kubow et al., 2014; Barnard-Kubow and Galloway, 2017). As observed in *S. nutans*, d_N/d_S values appeared to be particularly high in

plastid genes encoding subunits involved in plastid gene expression machinery.

4.2. Plastid-nuclear coevolution in Silene nutans lineages

Excess of non-synonymous substitutions in plastid genes of *S. nutans*, mainly due to relaxed selection, could impose strong selective pressures on the nuclear genes within lineages and within genomic complexes to maintain plastid-nuclear co-adaptation (Sloan et al., 2018). Evidence of coevolution between plastid and nuclear genes has been reported in several plant species (Ferreira de Carvalho et al., 2019; Moison et al., 2010; Rockenbach et al., 2016; Schmitz-Linneweber et al., 2005; Sharbrough et al., 2017; Sloan et al., 2014b; Weng et al., 2016; Williams et al., 2019; Zhang et al., 2015). Generally, this coevolution relies on parallel patterns of substitution accumulation between plastid and nuclear genes whose gene products are targeted to the plastid, with a high number of substitutions in one of the two genomic compartments, and signatures of positive selection on the other one, to ensure the maintenance of co-adaptation between mutated genes and the correct functioning of the plastid complex (Postel and Touzet, 2020). We identified parallel patterns of non-synonymous substitution accumulation between nuclear and plastid genes in *S. nutans*, within each plastid complex and lineage.

Disruption of co-adaptation between nuclear and plastid genes has been previously described in other plant systems and generally leads to impaired hybrid phenotypes exhibiting chlorosis and variegation and/or hybrid mortality, depending on the lineage used as the maternal parent (reviewed in Postel and Touzet, 2020). Asymmetric postzygotic reproductive isolation has been identified between W1 and E1 lineages of *S. nutans* using controlled reciprocal crosses (Martin et al., 2017). In addition, diallelic crosses conducted between the four studied lineages of *S. nutans* showed a large proportion of chlorotic or partially chlorotic hybrid progeny, and high hybrid seedling mortality, especially when E1 and W2 lineages were the maternal parents (Van Rossum et al. 2018, unpublished results). Hybrid juvenile mortality rate after 5 weeks of growth was 0.97 and 0.83 when E1 and W2 were the maternal lineages, and 0.50 and 0.23 when W1 and W3 were the mother, respectively (Van Rossum et al., unpublished results). These findings are consistent with our observations that E1 and W2 showed accumulation of substitutions in the plastid and nuclear genes and nuclear substitutions under positive selection, suggesting that these lineages contain the most functionally divergent and incompatible plastid genomes, causing PNIs in their hybrid progeny. Barnard-Kubow et al. (2017) reported a similar pattern for between-population hybrids of *C. americanum*, with higher hybrid mortality and chlorosis when populations with highly divergent plastid genomes were used as maternal lineages. In this system, PNIs have been put forward to explain the reproductive isolation (Barnard-Kubow et al., 2017; Barnard-Kubow and Galloway, 2017). Asymmetric reproductive isolation likely due to cytonuclear incompatibilities has also been described in *Oenothera* (Greiner et al., 2011), *Pelargonium* (Metzlaf et al., 1982; Weihe et al., 2009), and *Pisum* (Bogdanova et al., 2018, 2012; Bogdanova and Kosterin, 2007).

4.3. Are cytochrome b6/f and plastid ribosome possibly involved in PNI?

Disruption of co-adaptation between nuclear and plastid genes within a plastid complex leads to the malfunction of this complex. This malfunction often has physiological consequences, visible at the phenotypic level, and so hybrid phenotypes can give insight into the genetic location of the PNIs (Massouh et al., 2016; Yao and Cohen, 2000). For example, when leaves are almost entirely white, dysfunction of plastid expression machinery is suspected, while pale yellow leaves indicate a deficiency in chlorophyll and malfunction of the photosynthetic process (Liebers et al., 2017; Massouh et al., 2016; Yao and Cohen, 2000). Hybrid progeny between *S. nutans* lineages suffering from chlorosis exhibit pale yellow cotyledons rather than white ones (Martin et al., 2017; Van Rossum et al., unpublished data), suggesting a defect in one or several photosynthetic plastid complexes rather than a dysfunction of the plastid gene expression machinery (Li et al., 2019; Liebers et al., 2017).

Regarding our results, one good candidate for explaining the (partially) chlorotic hybrid phenotypes caused by PNIs is cytochrome b6/f. This plastid complex is directly involved in the photosynthetic process as it manages the electron transport chain between PSI and PSII (Malone et al., 2019). We found non-synonymous substitutions on the plastid genes encoding cytochrome b6/f (*petA* and *petD*) as well as on nuclear genes (mostly on *petM*). In particular, *petA* and *petM* exhibited parallel patterns of non-synonymous substitution accumulation in E1 and W2 lineages and our RELAX results highlighted a pattern of coevolution, at least between *petM* and *petA* within the cytochrome b6/f (Table S4). These two genes are known to be in physical interaction (Forsythe et al., 2019; Malone et al., 2019). Disruption of co-adaptation between these two genes, in hybrids with E1 or W2 lineages as maternal parents, could lead to the observed pale-yellow phenotypes.

A strong coevolution pattern was also identified between genes encoding the plastid ribosome of *S. nutans*. Knock-out or dysfunction of one of these genes can lead to impaired, potentially non-viable, mutant phenotypes (Tiller and Bock, 2014). The mutations identified in ribosomal plastid genes could have important functional consequences and reinforce the need for compensatory evolution of the nuclear genes to maintain the function of the plastid ribosome. Whether the plastid genes or the nuclear genes evolved in response to mutation accumulation in plastid or nuclear genomes remains unclear. Signature of positive selection, often considered as an indication of a compensatory dynamic to maintain co-adaptation (Greiner and Bock, 2013; Levin, 2003; Sloan et al., 2018), was observed in both genomic compartments. Tiller and Bock (2014) hypothesized that environmental changes affect translational activity of the plastid and generate a signal to modify leaf morphology and therefore photosynthesis performance. Accordingly, a recent study on *Brassica campestris* ssp. *pekinensis* identified a missense mutation in a ribosomal plastid gene (*rps4*) causing aberrant rRNA processing, which affected plastid translation and resulted in chlorophyll deficiency and reduced plant growth (Tang et al., 2018). Through their indirect role in photosynthesis, plastid ribosomal genes could be a target for positive selection which could lead to the fixation of adaptive mutations. Besides, a phylogenomic study across angiosperms found that genes involved in protein homeostasis exhibited a pattern of coevolution between plastid and nuclear genomes, suggesting recurrent bouts of selection on the plastid proteostasis systems, e.g., ribosomes (Forsythe et al., 2021). Further analyses based on the crystallographic structure of the plastid ribosome of *S. nutans* could give clues to the impact of each mutation on the protein-protein interactions network and on the whole structure of the plastid ribosome (Sharma et al., 2007).

The present study focused on coding sequences of genes encoding subunits of plastid complexes. Recent studies have shown that PNI could be also due to variations occurring in regulating sequences of plastid genes (Schmitz-Linneweber et al., 2005; Zupok et al., 2021). In fact, we found SNPs at 500 bp upstream of coding sequences (data not shown), but further analyses will be needed to survey gene expression. To do so, non-viable chlorotic hybrids should be rescued, possibly using media supplemented by sugar (Kühn et al., 2015). We acknowledge that some plastid genes that were excluded from our analyses could play a role in PNI (see Material and Methods), especially if the fact that we could not analyze them was due to their fast-evolutionary rate. For example, it was observed that CLP and ACCase complexes with fast-evolving plastid genes exhibited a strong pattern of coevolution with their nuclear counterparts, which could result in PNI (Forsythe et al., 2021; Rockenbach et al., 2016; Williams et al., 2019).

4.4. A link with gynodioecy?

The use of genomic and transcriptomic data enabled us to assess the

evolutionary dynamics of the plastid and nuclear genomes of *S. nutans* lineages, relying on the necessary coevolution between these two genomes for proper cell functioning. Plastid genomes of *S. nutans* exhibited high non-synonymous genetic diversity. It has been suggested that the gynodioecious mating system of *S. nutans* could have favored the speciation process (Martin et al., 2017). This reproductive system implies the presence of sterilizing mitochondrial genomes, leading to male sterility, and to male-fertility restoration by nuclear genes (Chase, 2007; Gouyon et al., 1991). Plastid and mitochondrial genomes are in tight linkage disequilibrium. Therefore, common evolutionary mechanisms may act on plastid and mitochondrial genomes (Olson and Mccauley, 2002). The specific evolutionary dynamics of the mitochondrial genome in this gynodioecious species could have impacted and dragged the co-transmitted plastid genome. Indeed, the selection of male-sterile mitochondrial genomes, with male-sterile plants exhibiting a higher female fitness (Frank, 1989), could have produced a pattern of linked selection on the co-transmitted plastid genomes. This would favor the fixation of mildly deleterious mutations in the plastid genome, subsequently launching the process of coevolution in the nuclear genome.

The authors declare that they have no known competing financial interests or personal relationships that could have appeared to influence the work reported in this paper.

CRediT authorship contribution statement

Zoé Postel: Investigation, Data curation, Formal analysis, Visualization, Writing – original draft. **Céline Poux:** Formal analysis, Methodology, Supervision, Writing – review & editing. **Sophie Gallina:** Conceptualization, Resources, Software. **Jean-Stéphane Varré:** Conceptualization. **Cécile Godé:** Resources. **Eric Schmitt:** Resources. **Etienne Meyer:** Formal analysis, Writing – review & editing. **Fabienne Van Rossum:** Resources, Writing – review & editing. **Pascal Touzet:** Conceptualization, Funding acquisition, Project administration, Supervision, Writing – original draft.

Declaration of Competing Interest

The authors declare that they have no known competing financial interests or personal relationships that could have appeared to influence the work reported in this paper.

Acknowledgements

This research was funded by the Agence Nationale de la Recherche (ANR-11-BSV7-013-03, TRANS), the Région Hauts-de-France, and the Ministère de l'Enseignement Supérieur et de la Recherche (CPER Climibio), and the European Fund for Regional Economic Development, and the Région Hauts-de-France and the Ministère de l'Enseignement Supérieur et de la Recherche for ZP's PhD grant. We wish to thank Camille Roux for his help in the elaboration of the scripts and Dan Sloan for discussion about transit peptide analyses.

Data accessibility

All plastid reads of *S. nutans* lineages were deposited in NCBI (PRJNA745523). Scripts are available at https://github.com/ZoePos/Variants-dectections.

Appendix A. Supplementary data

Supplementary data to this article can be found online at https://doi.org/10.1016/j.ympev.2022.107436.

References

Bankevich, A., Nurk, S., Antipov, D., Gurevich, A.A., Dvorkin, M., Kulikov, A.S., Lesin, V. M., Nikolenko, S.I., Pham, S., Prjibelski, A.D., Pyshkin, A.V., Sirotkin, A.V., Vyahhi, N., Tesler, G., Alekseyev, M.A., Pevzner, P.A., 2012. SPAdes: A new genome assembly algorithm and its applications to single-cell sequencing. J. Comput. Biol. 19 (5), 455–477. https://doi.org/10.1089/cmb.2012.0021.

Barnard-Kubow, K.B., Galloway, L.F., 2017. Variation in reproductive isolation across a species range. Ecol. Evol. 7 (22), 9347–9357. https://doi.org/10.1002/ece3.3400.

Barnard-Kubow, K.B., McCoy, M.A., Galloway, L.F., 2017. Biparental chloroplast inheritance leads to rescue from cytonuclear incompatibility. New Phytol. 213 (3), 1466–1476. https://doi.org/10.1111/nph.14222.

Barnard-Kubow, K.B., Sloan, D.B., Galloway, L.F., 2014. Correlation between sequence divergence and polymorphism reveals similar evolutionary mechanisms acting across multiple timescales in a rapidly evolving plastid genome. BMC Evol. Biol. 14, 1–10. https://doi.org/10.1186/s12862-014-0268-y.

Bateman, A., 2019. UniProt: A worldwide hub of protein knowledge. Nucleic Acids Res. 47, D506–D515. https://doi.org/10.1093/nar/gky1049.

Bogdanova, V.S., 2020. Genetic and Molecular Genetic Basis of Nuclear-Plastid Incompatibilities. Plants 9, 1–17.

Bogdanova, V.S., Galieva, E.R., Yadrikhinskiy, A.K., Kosterin, O.E., 2012. Inheritance and genetic mapping of two nuclear genes involved in nuclear-cytoplasmic incompatibility in peas (*Pisum sativum* L.). Theor. Appl. Genet. 124 (8), 1503–1512. https://doi.org/10.1007/s00122-012-1804-z.

Bogdanova, V.S., Kosterin, O.E., 2007. Hybridization barrier between *Pisum fulvum* Sibth. et Smith and *P. sativum* L. is partly due to nuclear-chloroplast incompatibility. Pisum Genet. 39, 8–9.

Bogdanova, V.S., Mglinets, A.V., Shatskaya, N.V., Kosterin, O.E., Solovyev, V.I., Vasiliev, G.V., 2018. Cryptic divergences in the genus *Pisum* L. (peas), as revealed by phylogenetic analysis of plastid genomes. Mol. Phylogenet. Evol. 129, 280–290. https://doi.org/10.1016/j.ympev.2018.09.002.

Budar, F., Roux, F., 2011. The role of organelle genomes in plant adaptation: time to get to work! Plant Signal Behav. 6 (5), 635–639.

Burton, R.S., Pereira, R.J., Barreto, F.S., 2013. Cytonuclear Genomic Interactions and Hybrid Breakdown. Annu. Rev. Ecol. Evol. Syst. 44 (1), 281–302. https://doi.org/10.1146/annurev-ecolsys-110512-135758.

Chase, C.D., 2007. Cytoplasmic male sterility: a window to the world of plant mitochondrial-nuclear interactions. Trends Genet. 23 (2), 81–90. https://doi.org/10.1016/j.tig.2006.12.004.

Christian, R.W., Hewitt, S.L., Roalson, E.H., Dhingra, A., 2020. Genome-Scale Characterization of Predicted Plastid-Targeted Proteomes in Higher Plants. Sci. Rep. 10, 1–22. https://doi.org/10.1038/s41598-020-64670-5.

Christie, J.R., Beekman, M., 2017. Uniparental inheritance promotes adaptive evolution in cytoplasmic genomes. Mol. Biol. Evol. 34, 677–691. https://doi.org/10.1093/molbev/msw266.

Cruickshank, T.E., Hahn, M.W., 2014. Reanalysis suggests that genomic islands of speciation are due to reduced diversity, not reduced gene flow. Mol. Ecol. 23 (13), 3133–3157. https://doi.org/10.1111/mec.12796.

Drouin, G., Daoud, H., Xia, J., 2008. Relative rates of synonymous substitutions in the mitochondrial, chloroplast and nuclear genomes of seed plants. Mol. Phylogenet. Evol. 49 (3), 827–831. https://doi.org/10.1016/j.ympev.2008.09.009.

Ferreira de Carvalho, J., Lucas, J., Deniot, G., Falentin, C., Filangi, O., Gilet, M., Legeai, F., Lode, M., Morice, J., Trotoux, G., Aury, J.-M., Barbe, V., Keller, J., Snowdon, R., He, Z., Denoeud, F., Wincker, P., Bancroft, I., Chèvre, A.-M., Rousseau-Gueutin, M., 2019. Cytonuclear interactions remain stable during allopolyploid evolution despite repeated whole-genome duplications in *Brassica*. Plant J. 98 (3), 434–447. https://doi.org/10.1111/tpj.14228.

Forsythe, E., Williams, A.M., Sloan, D., 2021. Genome-wide signatures of plastid-nuclear coevolution point to repeated perturbations of plastid proteostasis systems across angiosperms. Plant Cell 33, 980–997. https://doi.org/10.1093/plcell/koab021.

Forsythe, E.S., Sharbrough, J., Havird, J.C., Warren, J.M., Sloan, D.B., Chaw, S.M., 2019. CyMIRA: The Cytonuclear Molecular Interactions Reference for *Arabidopsis*. Genome Biol. Evol. 11, 2194–2202. https://doi.org/10.1093/gbe/evz144.

Frank, S.A., 1989. The evolutionary dynamics of cytoplasmic male sterility. Am. Nat. 133 (3), 345–376.

Gayral, P., Melo-Ferreira, J., Glémin, S., Bierne, N., Carneiro, M., Nabholz, B., Lourenco, J.M., Alves, P.C., Ballenghien, M., Faivre, N., Belkhir, K., Cahais, V., Loire, E., Bernard, A., Galtier, N., Welch, J.J., 2013. Reference-Free Population Genomics from Next- Generation Transcriptome Data and the Vertebrate – Invertebrate Gap. PLoS Genet. 9 (4), e1003457. https://doi.org/10.1371/journal.pgen.1003457.

Gouy, M., Guindon, S., Gascuel, O., 2010. Sea view version 4: A multiplatform graphical user interface for sequence alignment and phylogenetic tree building. Mol. Biol. Evol. 27 (2), 221–224. https://doi.org/10.1093/molbev/msp259.

Gouyon, P.H., Vichot, F., Van Damme, J.M.M., 1991. Nuclear-cytoplasmic male sterility: single-point equilibria versus limit cycles. Am. Nat. 137, 498–514. https://doi.org/10.1086/285179.

Greiner, S., Bock, R., 2013. Tuning a ménage à trois: Co-evolution and co-adaptation of nuclear and organellar genomes in plants. BioEssays 35 (4), 354–365. https://doi.org/10.1002/bies.201200137.

Greiner, S., Rauwolf, U., Meurer, J., Herrmann, R.G., 2011. The role of plastids in plant speciation. Mol. Ecol. 20, 671–691. https://doi.org/10.1111/j.1365-294X.2010.04984.x.

Greiner, S., Sobanski, J., Bock, R., 2015. Why are most organelle genomes transmitted maternally? BioEssays 37 (1), 80–94. https://doi.org/10.1002/bies.201400110.

Guindon, S., Dufayard, J., Lefort, V., 2010. New Algorithms and Methods to Estimate Maximim-Likelihood Phylogenies Assessing the Performance of PhyML 3.0. Syst. Biol. 59, 307–321.
Hooper, C.M., Castleden, I.R., Tanz, S.K., Aryamanesh, N., Millar, A.H., 2017. SUBA4: The interactive data analysis centre for *Arabidopsis* subcellular protein locations. Nucleic Acids Res. 45 (D1), D1064–D1074. https://doi.org/10.1093/nar/gkw1041.
Hubisz, M.J., Pollard, K.S., Siepel, A., 2011. PHAST and RPHAST: Phylogenetic analysis with space/time models. Brief. Bioinform. 12 (1), 41–51. https://doi.org/10.1093/bib/bbq072.
Jafari, F., Zarre, S., Gholipour, A., Eggens, F., Rabeler, R.K., Oxelman, B., 2020. A new taxonomic backbone for the infrageneric classification of the species-rich genus *Silene* (Caryophyllaceae). Syst. Phylogeny 69 (2), 337–368. https://doi.org/10.1002/tax.12230.
Jansen, R.K., Cai, Z., Raubeson, L.A., Daniell, H., dePamphilis, C.W., Leebens-Mack, J., Muller, K.F., Guisinger-Bellian, M., Haberle, R.C., Hansen, A.K., Chumley, T.W., Lee, S.-B., Peery, R., McNeal, J.R., Kuehl, J.V., Boore, J.L., 2007. Analysis of 81 genes from 64 plastid genomes resolves relationships in angiosperms and identifies genome-scale evolutionary patterns. PNAS 104 (49), 19369–19374. https://doi.org/10.1073/pnas.0709121104.
Juan, J., Armenteros, A., Salvatore, M., Emanuelsson, O., Winther, O., Heijne, G.V., Elofsson, A., Nielsen, H., 2019. Detecting sequence signals in targeting peptides using deep learning. Life Sci. Alliance e201900429 2, 1–14. https://doi.org/10.26508/lsa.201900429.
Kühn, K., Obata, T., Feher, K., Bock, R., Fernie, A.R., Meyer, E.H., 2015. Complete Mitochondrial Complex I Deficiency Induces an Up-Regulation of Respiratory Fluxes That Is Abolished by Traces of Functional Complex I. Plant Physiol. 168 (4), 1537–1549. https://doi.org/10.1104/pp.15.00589.
Lefort, V., Longueville, J., Gascuel, O., 2017. SMS : Smart Model Selection in PhyML. Mol. Biol. Evol. 34, 2422–2424. https://doi.org/10.1093/molbev/msx149.
Levin, D.A., 2003. The cytoplasmic factor in plant speciation. Syst. Bot. 28, 5–11. https://doi.org/10.1043/0363-6445-28.1.5.
Li, M., Hensel, G., Mascher, M., Melzer, M., Budhagatapalli, N., Rutten, T., Himmelbach, A., Beier, S., Korzun, V., Kumlehn, J., Börner, T., Stein, N., 2019. Leaf Variegation and Impaired Chloroplast Development Caused by a Truncated CCT Domain Gene in *albostrians* Barley. Plant Cell 31 (7), 1430–1445. https://doi.org/10.1105/tpc.19.00132.
Liebers, M., Grübler, B., Chevalier, F., Lerbs-mache, S., Merendino, L., Blanvillain, R., Pfannschmidt, T., 2017. Regulatory Shifts in Plastid Transcription Play a Key Role in Morphological Conversions of Plastids during Plant Development. Front. Plant Sci. 8, 1–8. https://doi.org/10.3389/fpls.2017.00023.
Malone, L.A., Qian, P., Mayneord, G.E., Hitchcock, A., Farmer, D.A., Thompson, R.F., Swainsbury, D.J.K., Ranson, N.A., Hunter, C.N., Johnson, M.P., 2019. Cryo-EM structure of the spinach cytochrome b6f complex at 3.6 Å resolution. Nature 575, 535–539. https://doi.org/10.1038/s41586-019-1746-6.
Martin, H., Touzet, P., Dufay, M., Godé, C., Schmitt, E., Lahiani, E., Delph, L.F., Van Rossum, F., 2017. Lineages of *Silene nutans* developed rapid, strong, asymmetric postzygotic reproductive isolation in allopatry. Evolution 71 (6), 1519–1531. https://doi.org/10.1111/evo.13245.
Martin, H., Touzet, P., Van Rossum, F., Delalande, D., Arnaud, J.-F., 2016. Phylogeographic pattern of range expansion provides evidence for cryptic species lineages in *Silene nutans* in Western Europe. Heredity 116 (3), 286–294. https://doi.org/10.1038/hdy.2015.100.
Massouh, A., Schubert, J., Yaneva-Roder, L., Ulbricht-Jones, E.S., Zupok, A., Johnson, M. T.J., Wright, S.I., Pellizzer, T., Sobanski, J., Bock, R., Greiner, S., 2016. Spontaneous chloroplast mutants mostly occur by replication slippage and show a biased pattern in the plastome of *Oenothera*. Plant Cell 28 (4), 911–929. https://doi.org/10.1105/tpc.15.00879.
Matute, D.R., Cooper, B.S., 2021. Comparative studies on speciation : 30 years since Coyne and Orr. Evolution 75, 764–778. https://doi.org/10.1111/evo.14181.
Metzlaf, M., Pohlheim, F., Borner, T., Hagemann, R., 1982. Hybrid variegation in the genus *Pelargonium*. Curr. Genet. 5 (3), 245–249. https://doi.org/10.1007/BF00391813.
Moison, M., Roux, F., Quadrado, M., Duval, R., Ekovich, M., Lê, D.H., Verzaux, M., Budar, F., 2010. Cytoplasmic phylogeny and evidence of cyto-nuclear co-adaptation in *Arabidopsis thaliana*. Plant J. 63, 728–738. https://doi.org/10.1111/j.1365-313X.2010.04275.x.
Muyle, A., Martin, H., Zemp, N., Mollion, M., Gallina, S., Tavares, R., Silva, A., Bataillon, T., Widmer, A., Glémin, S., Touzet, P., Marais, G.A.B., Stephen, W., 2021. Dioecy Is Associated with High Genetic Diversity and Adaptation Rates in the Plant Genus *Silene*. Mol. Biol. Evol. 38 (3), 805–818. https://doi.org/10.1093/molbev/msaa229.
Noé, L., Kucherov, G., 2005. YASS : enhancing the sensitivity of DNA similarity search. Nucleic Acids Res. 33, 540–543. https://doi.org/10.1093/nar/gki478.
Olson, M.S., Mccauley, D.E., 2002. Mitochondrial DNA diversity, population structure, and gender association in the gynodioecious plant *Silene vulgaris*. Evolution 56 (2), 253–262.
Oughtred, R., Stark, C., Breitkreutz, B.J., Rust, J., Boucher, L., Chang, C., Kolas, N., O'Donnell, L., Leung, G., McAdam, R., Zhang, F., Dolma, S., Willems, A., Coulombe-Huntington, J., Chatr-Aryamontri, A., Dolinski, K., Tyers, M., 2019. The BioGRID interaction database: 2019 update. Nucleic Acids Res. 47, D529–D541. https://doi.org/10.1093/nar/gky1079.
Page, J.T., Liechty, Z.S., Huynh, M.D., Udall, J.A., 2014. BamBam: Genome sequence analysis tools for biologists. BMC Res. Notes 7, 1–5. https://doi.org/10.1186/1756-0500-7-829.
Postel, Z., Touzet, P., 2020. Cytonuclear genetic incompatibilities in plant speciation. Plants 9, 1–21. https://doi.org/10.3390/plants9040487.
Rand, D.M., Haney, R.A., Fry, A.J., 2004. Cytonuclear coevolution: The genomics of cooperation. Trends Ecol. Evol. 19 (12), 645–653. https://doi.org/10.1016/j.tree.2004.10.003.
Ranwez, V., Harispe, S., Delsuc, F., Douzery, E.J.P., Murphy, W.J., 2011. MACSE: Multiple Alignment of Coding SEquences accounting for frameshifts and stop codons. PLoS One 6 (9), e22594. https://doi.org/10.1371/journal.pone.0022594.
Rockenbach, K., Havird, J.C., Grey Monroe, J., Triant, D.A., Taylor, D.R., Sloan, D.B., 2016. Positive selection in rapidly evolving plastid-nuclear enzyme complexes. Genetics 204, 1507–1522. https://doi.org/10.1534/genetics.116.188268.
Rozas, J., Ferrer-mata, A., S, J.C., Guirao-rico, S., Librado, P., Ramos-onsins, E., Alejandro, S.-G., 2017. DnaSP 6: DNA Sequence Polymorphism Analysis of Large Data Sets. Mol. Biol. Evol. 34, 3299–3302. https://doi.org/10.1093/molbev/msx248.
Schmitz-Linneweber, C., Kushnir, S., Babiychuk, E., Poltnigg, P., Herrmann, R.G., Maier, R.M., 2005. Pigment deficiency in nightshade/tobacco cybrids is caused by the failure to edit the plastid ATPase α-subunit mRNA. Plant Cell 17, 1815–1828. https://doi.org/10.1105/tpc.105.032474.
Sharbrough, J., Conover, J.L., Tate, J.A., Wendel, J.F., Sloan, D.B., 2017. Cytonuclear responses to genome doubling. Am. J. Bot. 104 (9), 1277–1280. https://doi.org/10.3732/ajb.1700293.
Sharma, M.R., Wilson, D.N., Datta, P.P., Barat, C., Schluenzen, F., Fucini, P., Agrawal, R. K., 2007. Cryo-EM study of the spinach chloroplast ribosome reveals the structural and functional roles of plastid-specific ribosomal proteins. PNAS 104 (49), 19315–19320. https://doi.org/10.1073/pnas.0709856104.
Siepel, A., Haussler, D., 2004. Phylogenetic Estimation of Context-Dependent Substitution Rates by Maximum Likelihood. Mol. Gen. Genet. 21, 468–488. https://doi.org/10.1093/molbev/msh039.
Sloan, D.B., Triant, D.A., Forrester, N.J., Bergner, L.M., Wu, M., Taylor, D.R., 2014a. A recurring syndrome of accelerated plastid genome evolution in the angiosperm tribe *Sileneae* (Caryophyllaceae). Mol. Phylogenet. Evol. 72, 82–89. https://doi.org/10.1016/j.ympev.2013.12.004.
Sloan, D.B., Triant, D.A., Wu, M., Taylor, D.R., 2014b. Cytonuclear interactions and relaxed selection accelerate sequence evolution in organelle ribosomes. Mol. Biol. Evol. 31, 673–682. https://doi.org/10.1093/molbev/mst259.
Sloan, D.B., Warren, J.M., Williams, A.M., Wu, Z., Abdel-Ghany, S.E., Chicco, A.J., Havird, J.C., 2018. Cytonuclear integration and co-evolution. Nat. Rev. Genet. 19 (10), 635–648. https://doi.org/10.1038/s41576-018-0035-9.
Szklarczyk, D., Gable, A.L., Lyon, D., Junge, A., Wyder, S., Huerta-Cepas, J., Simonovic, M., Doncheva, N.T., Morris, J.H., Bork, P., Jensen, L.J., Von Mering, C., 2019. STRING v11: Protein-protein association networks with increased coverage, supporting functional discovery in genome-wide experimental datasets. Nucleic Acids Res. 47, D607–D613. https://doi.org/10.1093/nar/gky1131.
Tang, X., Wang, Y., Zhang, Y., Huang, S., Liu, Z., Fei, D., Feng, H., 2018. A missense mutation of plastid RPS4 is associated with chlorophyll deficiency in Chinese cabbage (*Brassica campestris ssp. pekinensis*). BMC Plant Biol. 18, 1–11. https://doi.org/10.1186/s12870-018-1353-y.
Tiller, N., Bock, R., 2014. The translational apparatus of plastids and its role in plant development. Mol. Plant 7 (7), 1105–1120. https://doi.org/10.1093/mp/ssu022.
Tiller, N., Weingartner, M., Thiele, W., Maximova, E., Schöttler, M.A., Bock, R., 2012. The plastid-specific ribosomal proteins of *Arabidopsis thaliana* can be divided into non-essential proteins and genuine ribosomal proteins. Plant J. 69 (2), 302–316. https://doi.org/10.1111/j.1365-313X.2011.04791.x.
Turelli, M., Moyle, L.C., 2007. Asymmetric postmating isolation: Darwin's corollary to Haldane's rule. Genetics 176, 1059–1088. https://doi.org/10.1534/genetics.106.065979.
Van Rossum, F., Martin, H., Le Cadre, S., Brachi, B., Christenhusz, M.J.M., Touzet, P., 2018. Phylogeography of a widely distributed species reveals a cryptic assemblage of distinct genetic lineages needing separate conservation strategies. Perspect. Plant Ecol. Evol. Syst. 35, 44–51. https://doi.org/10.1016/j.ppees.2018.10.003.
Varadi, M., Berrisford, J., Deshpande, M., Nair, S.S., Gutmanas, A., Armstrong, D., Pravda, L., Al-Lazikani, B., Anyango, S., Barton, G.J., Berka, K., Blundell, T., Borkakoti, N., Dana, J., Das, S., Dey, S., Micco, P.D., Fraternali, F., Gibson, T., Helmer-Citterich, M., Hoksza, D., Huang, L.-C., Jain, R., Jubb, H., Kannas, C., Kannan, N., Koca, J., Krivak, R., Kumar, M., Levy, E.D., Madeira, F., Madhusudhan, M.S., Martell, H.J., MacGowan, S., McGreig, J.E., Mir, S., Mukhopadhyay, A., Parca, L., Paysan-Lafosse, T., Radusky, L., Ribeiro, A., Serrano, L., Sillitoe, I., Singh, G., Skoda, P., Svobodova, R., Tyzack, J., Valencia, A., Fernandez, E.V., Vranken, W., Wass, M., Thornton, J., Sternberg, M., Orengo, C., Velankar, S., 2020. PDBE-KB: A community-driven resource for structural and functional annotations. Nucleic Acids Res. 48 (D1), D344–D353. https://doi.org/10.1093/nar/gkz853.
Weihe, A., Apitz, J., Pohlheim, F., Salinas-Hartwig, A., Börner, T., 2009. Biparental inheritance of plastidial and mitochondrial DNA and hybrid variegation in *Pelargonium*. Mol. Genet. Genomics 282 (6), 587–593. https://doi.org/10.1007/s00438-009-0488-9.
Weng, M.-L., Ruhlman, T.A., Jansen, R.K., 2016. Plastid–nuclear interaction and accelerated coevolution in plastid ribosomal genes in Geraniaceae. Genome Biol. Evol. 8 (6), 1824–1838. https://doi.org/10.1093/gbe/evw115.
Wertheim, J.O., Murrell, B., Smith, M.D., Pond, S.L.K., Scheffler, K., 2015. RELAX : Detecting Relaxed Selection in a Phylogenetic Framework. Mol. Biol. Evol. 32, 820–832. https://doi.org/10.1093/molbev/msu400.
Williams, A.M., Friso, G., van Wijk, K.J., Sloan, D.B., 2019. Extreme variation in rates of evolution in the plastid Clp protease complex. Plant J. 98 (2), 243–259. https://doi.org/10.1111/tpj.14208.

Wolfe, K.H., Li, W.H., Sharp, P.M., 1987. Rates of nucleotide substitution vary greatly among plant mitochondrial, chloroplast, and nuclear DNAs. PNAS 84 (24), 9054–9058.

Yang, Z., 2007. PAML 4: Phylogenetic analysis by maximum likelihood. Mol. Biol. Evol. 24, 1586–1591. https://doi.org/10.1093/molbev/msm088.

Yao, J.-L., Cohen, D., 2000. Multiple gene control of plastome-genome incompatibility and plastid DNA inheritance in interspecific hybrids of *Zantedeschia*. Theor. Appl. Genet. 101 (3), 400–406. https://doi.org/10.1007/s001220051496.

Zhang, J., Ruhlman, T.A., Sabir, J., Blazier, J.C., Jansen, R.K., 2015. Coordinated rates of evolution between interacting plastid and nuclear genes in Geraniaceae. Plant Cell 27, 563–573. https://doi.org/10.1105/tpc.114.134353.

Zupok, A., Kozul, D., Schöttler, M.A., Niehörster, J., Garbsch, F., Liere, K., Fischer, A., Zoschke, R., Malinova, I., Bock, R., Greiner, S., 2021. A photosynthesis operon in the chloroplast genome drives speciation in evening primroses. Plant Cell koab155. https://doi.org/10.1093/plcell/koab155.